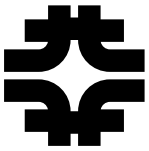

**Fermi National Accelerator Laboratory**

**FERMILAB-Pub-00/084-T**

# $B_{s,d}$ to $\ell^+\ell^-$ in a Two-Higgs-Doublet Model

Heather E. Logan and Ulrich Nierste

*Fermi National Accelerator Laboratory*
*P.O. Box 500, Batavia, Illinois 60510*

April 2000

Submitted to *Nuclear Physics B*

Operated by Universities Research Association Inc. under Contract No. DE-AC02-76CH03000 with the United States Department of Energy

FERMILAB-Pub-00/084-T, hep-ph/0004139

# $\mathrm{B_{s,d}} \to \ell^+\ell^-$ in a Two-Higgs-Doublet Model

*Heather E. Logan*[1] *and Ulrich Nierste*[1]
*Theoretical Physics Department, Fermilab, Batavia, IL 60510-0500, USA.*[2]

## Abstract

We compute the branching fractions of $B_{s,d} \to \ell^+\ell^-$ in the type-II two-Higgs-doublet model with large $\tan\beta$. We find that the parameters of the neutral Higgs sector of the two-Higgs-doublet model cancel in the result, so that the branching fractions depend only on the charged Higgs mass and $\tan\beta$. For large values of $\tan\beta$ and a charged Higgs mass above the bound from $b \to s\gamma$, we find that the branching fractions can be enhanced by up to an order of magnitude or suppressed by up to a factor of two compared to the Standard Model result. We point out that previous calculations in the literature are gauge-dependent due to the omission of an important diagram, which gives the dominant contribution in the 't Hooft-Feynman gauge. We have analyzed in detail the region of the $(M_{H^+}, \tan\beta)$ plane to be probed by searches for $B_s \to \mu^+\mu^-$ in Run II of the Tevatron. Since the branching fraction increases like $\tan^4\beta$, this decay mode is complementary to $b \to s\gamma$ and efficiently probes the large $\tan\beta$ region. For $\tan\beta = 60$, an integrated luminosity of 20 fb$^{-1}$ in an extended Run II will probe charged Higgs masses up to 260 GeV, if the background to $B_s \to \mu^+\mu^-$ is small. For the same value of $\tan\beta$, the LHC may be able to explore charged Higgs masses up to 1 TeV using this decay.

PACS: 13.20.He, 12.60.Fr, 14.80.Cp
Keywords: $B$, leptonic decay; Higgs particle, multiplet; Higgs particle, mass

---

## 1 Introduction

The ongoing and forthcoming high-statistics B-physics experiments at BaBar, BELLE, HERA-B, the Tevatron, and the LHC experiments ATLAS, CMS and LHCb [1] will

[1]electronic addresses: logan@fnal.gov, nierste@fnal.gov

[2]Fermilab is operated by Universities Research Association Inc. under contract no. DE-AC02-76CH03000 with the US Department of Energy

probe the flavor sector of the Standard Model (SM) with high precision. These experiments may reveal physics beyond the SM, and a substantial theoretical effort is devoted to calculating the observables that will be tested in various scenarios of new physics.

A common feature of all popular weakly-coupled extensions of the SM is an enlarged Higgs sector. In this paper we study the type-II two-Higgs-doublet model (2HDM), which has the same particle content and tree-level Yukawa couplings as the Higgs sector of the Minimal Supersymmetric Model (MSSM). If the ratio $\tan\beta$ of the two Higgs vacuum expectation values is large, the Yukawa coupling to $b$ quarks is of order one and large effects on $B$ decays are possible. Direct searches for the lightest neutral MSSM Higgs particle have begun to constrain the low $\tan\beta$ region in the MSSM, because the theoretically predicted mass range increases with $\tan\beta$. Hence observables allowing us to study the complementary region of large $\tan\beta$ are increasingly interesting. A further theoretical motivation to study the large $\tan\beta$ case is SO(10) grand unified theories [2]: they unify the top and bottom Yukawa couplings at high energies, corresponding to $\tan\beta$ of order 50.

The leptonic decay $B_{d'} \to \ell^+\ell^-$, where $d' = d$ or $s$ and $\ell = e$, $\mu$ or $\tau$, is especially well suited to the study of an enlarged Higgs sector with large $\tan\beta$. In the SM the decay amplitude suffers from a helicity-suppression factor of $m_\ell/m_b$, which is absent in the Higgs-mediated contribution. This helicity suppression factor numerically competes with the suppression factor of $(m_\ell/M_W)\tan\beta$ stemming from the Higgs Yukawa couplings to the final state leptons, so that one expects the new contributions in the 2HDM to be similar in size to those of the SM.

Earlier papers have already addressed the decay $B_{d'} \to \ell^+\ell^-$ in the 2HDM or the full MSSM [3–8]. Yet the presented results differ analytically and numerically substantially from each other, so that we have decided to perform a new analysis.

This paper is organized as follows. In section 2 we give a brief review of the type-II 2HDM. In section 3 we review the SM calculation of the decay $B_{d'} \to \ell^+\ell^-$ and describe our calculation of the relevant 2HDM diagrams. We finish section 3 by combining the results for the 2HDM diagrams and giving compact expressions for the branching fractions. In section 4 we compare our result with previous calculations. In section 5 we present a numerical analysis of our result and estimate the reach of future experiments. We present our conclusions in section 6. Finally the appendix contains a discussion of trilinear Higgs couplings.

# 2 The two-Higgs-doublet model

In this paper we study the type-II 2HDM. The model is reviewed in detail in ref. [9]. The 2HDM contains two complex SU(2) doublet scalar fields,

$$\Phi_1 = \begin{pmatrix} \phi_1^+ \\ \phi_1^0 \end{pmatrix}, \qquad \Phi_2 = \begin{pmatrix} \phi_2^+ \\ \phi_2^0 \end{pmatrix}, \tag{1}$$

which acquire the vacuum expectation values (vevs) $\langle \phi_i^0 \rangle = v_i$ and break the electroweak symmetry. The Higgs vevs $v_1$ and $v_2$ are constrained by the $W$ boson mass, $M_W^2 = \frac{1}{2}g^2(v_1^2 + v_2^2) = \frac{1}{2}g^2 v_{SM}^2$, where $v_{SM} = 174$ GeV is the SM Higgs vev. Their ratio is parameterized by $\tan\beta = v_2/v_1$.
Since in this paper we are not interested in CP-violating quantities, we assume CP is conserved by the Higgs sector for simplicity. The mass eigenstates are then given as follows. The charged Higgs states are

$$\begin{aligned} G^+ &= \phi_1^+ \cos\beta + \phi_2^+ \sin\beta \\ H^+ &= -\phi_1^+ \sin\beta + \phi_2^+ \cos\beta, \end{aligned} \tag{2}$$

and their hermitian conjugates. The CP-odd states are

$$\begin{aligned} G^0 &= \phi_1^{0,i} \cos\beta + \phi_2^{0,i} \sin\beta \\ A^0 &= -\phi_1^{0,i} \sin\beta + \phi_2^{0,i} \cos\beta, \end{aligned} \tag{3}$$

where we use the notation $\phi_i^0 = v_i + \frac{1}{\sqrt{2}}(\phi_i^{0,r} + i\phi_i^{0,i})$ for the real and imaginary parts of $\phi_i^0$. The would-be Goldstone bosons $G^\pm$ and $G^0$ are eaten by the $W$ and $Z$ bosons. The CP-even states mix by an angle $\alpha$ giving two states,

$$\begin{aligned} H^0 &= \phi_1^{0,r} \cos\alpha + \phi_2^{0,r} \sin\alpha \\ h^0 &= -\phi_1^{0,r} \sin\alpha + \phi_2^{0,r} \cos\alpha. \end{aligned} \tag{4}$$

In order to avoid large flavor-changing neutral Higgs interactions we require natural flavor conservation [10]. We impose the discrete symmetry $\Phi_1 \to -\Phi_1$, $\Phi_2 \to \Phi_2$ (which is softly broken by dimension-two terms in the Higgs potential), with the SU(2) singlet fermion fields transforming as $d \to -d$, $u \to u$, $e \to -e$. These transformation rules define the type-II 2HDM and determine the Higgs-fermion Yukawa couplings. The Yukawa terms in the Lagrangian are:

$$\mathcal{L}_{\rm Yuk} = -Y_d \bar{Q} \Phi_1 d - Y_u \bar{Q} \Phi_2^c u - Y_l \bar{L} \Phi_1 e + \text{h.c.} \tag{5}$$

where $\Phi^c = i\tau_2\Phi^*$. Down-type quarks and charged leptons (up-type quarks) are given mass by their couplings to $\Phi_1$ ($\Phi_2$).
Most of the Higgs couplings needed in our calculation are given in ref. [9]. In addition we must consider the trilinear $H^+H^-H$ couplings ($H = h^0, H^0$) which were first given in ref. [5] and are discussed in appendix A.

# 3 Effective hamiltonian for $\mathrm{B} \to \ell^+\ell^-$

The decay $B_{d'} \to \ell^+\ell^-$ proceeds through loop diagrams and is of fourth order in the weak coupling. In both the SM and 2HDM, the contributions with a top quark in the loop are dominant, so that one may describe the decay at low energies of order $m_b$ by a local $\bar{b}d'\bar{\ell}\ell$ coupling via the effective hamiltonian,

$$H = \frac{G_F}{\sqrt{2}}\frac{\alpha_{EM}}{2\pi\sin^2\theta_W}\xi_t\left[C_S Q_S + C_P Q_P + C_A Q_A\right]. \tag{6}$$

Here $G_F$ is the Fermi constant, $\alpha_{EM}$ is the electromagnetic fine structure constant and $\theta_W$ is the Weinberg angle. The CKM elements are contained in $\xi_t = V_{tb}^* V_{td'}$. The operators in (6) are

$$Q_S = m_b\,\bar{b}P_L d'\,\bar{\ell}\ell, \qquad Q_P = m_b\,\bar{b}P_L d'\,\bar{\ell}\gamma_5\ell, \qquad Q_A = \bar{b}\gamma^\mu P_L d'\,\bar{\ell}\gamma_\mu\gamma_5\ell, \tag{7}$$

where $P_L = (1-\gamma_5)/2$ is the left-handed projection operator. We have neglected the right-handed scalar quark operators because they give contributions only proportional to the $d'$ mass. The vector leptonic operator $\bar{\ell}\gamma^\mu\ell$ does not contribute to $B_{d'} \to \ell^+\ell^-$, because it gives zero when contracted with the $B_{d'}$ momentum. Finally, no operators involving $\sigma_{\mu\nu} = i\left[\gamma_\mu, \gamma_\nu\right]/2$ contribute to $B_{d'} \to \ell^+\ell^-$.
Because $m_b \ll M_W, m_t, M_{H^+}$, there are highly separated mass scales in the decay $B_{d'} \to \ell^+\ell^-$. Short-distance QCD corrections can therefore contain large logarithms like $\log(m_b/M_W)$, which must be summed to all orders in perturbation theory with the help of renormalization group techniques. The calculation of the diagrams in the full high-energy theory gives the initial condition for the Wilson coefficients at a high renormalization scale $\mu$ on the order of the heavy masses in the loops. The hadronic matrix elements, however, are calculated at a low scale $\mu = \mathcal{O}(m_b)$ characteristic of the $B_{d'}$ decay. The renormalization group evolution down to this low scale requires the solution of the renormalization group equations of the operators $Q_A$, $Q_S$ and $Q_P$. Yet the operator $Q_A$ has zero anomalous dimension because it is a $(V-A)$ quark current, which is conserved in the limit of vanishing quark masses. Similarly, the operators $Q_S$ and $Q_P$

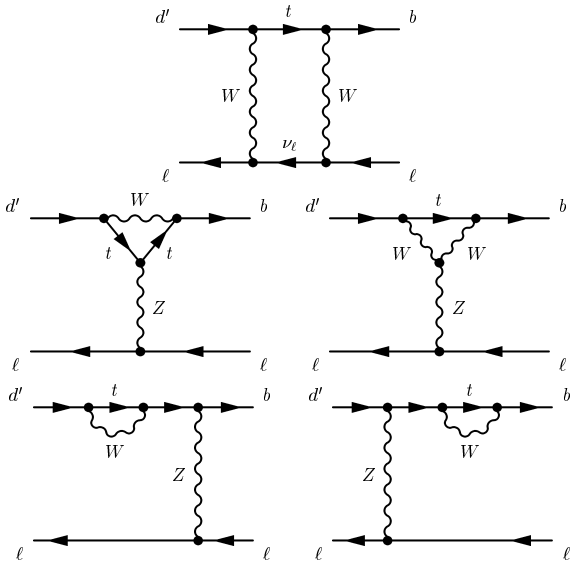


Figure 1: Dominant SM diagrams.

have zero anomalous dimension because the anomalous dimensions of the quark mass $m_b(\mu)$ and the (chiral) scalar current $\bar{b}P_L d'(\mu)$ add to zero. Hence the renormalization group evolution is trivial: if the bottom quark mass in $Q_S$ and $Q_P$ is normalized at a low scale $\mu = \mathcal{O}(m_b)$, then no large logarithms appear in the effective hamiltonian or in the decay rate.

In the SM, the dominant contributions to this decay come from the $W$ box and $Z$ penguin diagrams shown in fig. 1. These diagrams were first calculated in [11] and give a non-negligible contribution only to the Wilson coefficient $C_A$. There is no contribution from a photonic penguin because of the photon's pure vector coupling to leptons. There are also contributions to the Wilson coefficient $C_S$ from a SM Higgs penguin [12] and to the Wilson coefficient $C_P$ from the would-be neutral Goldstone boson penguin [13], but these contributions to the amplitude are suppressed by a factor of $m_b^2/M_W^2$ relative to the dominant contributions and can be ignored.

The SM decay amplitude is then given by the Wilson coefficient [11]

$$C_A = 2Y(x_t), \tag{8}$$

where $x_t = m_t^2(m_t)/M_W^2 = 4.27 \pm 0.26$ and $m_t$ is evaluated in the $\overline{\rm MS}$ scheme at $\mu = m_t$, giving $m_t(m_t) = 166$ GeV. The function $Y(x_t)$ is given by $Y(x_t) = Y_0(x_t) +$

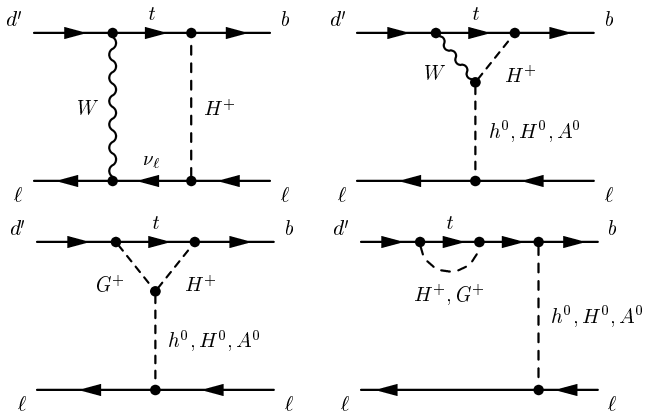


Figure 2: Dominant diagrams in the 2HDM with large $\tan\beta$.

$\frac{\alpha_s}{4\pi}Y_1(x_t)$, where $Y_0(x_t)$ gives the leading order (LO) contribution calculated in [11] and $Y_1(x_t)$ incorporates the next-to-leading (NLO) QCD corrections and is given in [14]. The NLO corrections increase $Y(x_t)$ by about 3%, if $m_t$ is normalized at $\mu = m_t$. Numerically,

$$Y(x_t) = 0.997 \left[\frac{m_t(m_t)}{166\ \mathrm{GeV}}\right]^{1.55}, \tag{9}$$

where we have parameterized the dependence on the running top quark mass in the $\overline{\mathrm{MS}}$ scheme.

We limit our consideration to the case of large $\tan\beta$, for which the 2HDM contributions to this decay are significant. In the large $\tan\beta$ limit, the Wilson coefficients $C_P$ and $C_S$ receive sizeable contributions from the box diagram involving $W$ and $H^+$ and the penguins and fermion self-energy diagrams with neutral Higgs boson exchange shown in fig. 2. There are no new contributions to $C_A$ in the 2HDM, which therefore retains its SM value.

We have calculated the individual diagrams explicitly in a general $R_\xi$ gauge, keeping only the terms proportional to $\tan^2\beta$. Although each diagram that involves a $W^\pm$ or $G^\pm$ boson is gauge-dependent, their sum is gauge-independent. For compactness, we give the results of the individual diagrams below in the 't Hooft-Feynman gauge.

## 3.1 Box diagram

The box diagram in fig. 2 gives the following contribution to $C_S$ and $C_P$:

$$C_S^{box} = C_P^{box} = \frac{m_\ell}{2M_W^2} \tan^2\beta\, B_+(x_{H^+}, x_t)\,. \tag{10}$$

Here $x_{H^+} = M_{H^+}^2/M_W^2$ and $x_t$ was defined after (8) in terms of $m_t(m_t)$. Strictly speaking, in a LO calculation like ours, one is not sensitive to the renormalization scheme and we could equally well use the top quark pole mass in $x_t$. However, experience with NLO calculations in the SM [14] shows that with the definition of $m_t$ adopted here, higher-order QCD corrections are small in leptonic decays. Finally the loop function $B_+$ in (10) reads

$$B_+(x,y) = \frac{y}{x-y}\left[\frac{\log y}{y-1} - \frac{\log x}{x-1}\right]. \tag{11}$$

$B_+(x_{H^+}, x_t)$ also contains the contribution from internal up and charm quarks with $m_c = m_u = 0$ from the implementation of the GIM mechanism. The effect of a nonzero charm quark mass is negligibly small.

## 3.2 Penguins

The penguin diagram with $H^+$ and $W^+$ in the loop (see fig. 2) contributes

$$\begin{aligned} C_S^{peng,1} &= \frac{m_\ell}{2}\,\tan^2\beta\, P_+(x_{H^+}, x_t)\left[\frac{\sin^2\alpha}{M_{h^0}^2} + \frac{\cos^2\alpha}{M_{H^0}^2}\right], \\ C_P^{peng,1} &= \frac{m_\ell}{2}\,\tan^2\beta\, P_+(x_{H^+}, x_t)\,\frac{1}{M_{A_0}^2}. \end{aligned} \tag{12}$$

Here again all three quark flavors enter the result from the GIM mechanism, and the effect of nonzero charm quark mass is negligible. By contrast, in the penguin diagram involving $H^+$ and $G^+$ in the loop only the internal top quark contribution is relevant, because the coupling of $G^+$ to quarks is proportional to either of the quark masses and we neglect $m_s$. This diagram gives

$$\begin{aligned} C_S^{peng,2} &= -\frac{m_\ell}{2}\,\tan^2\beta\, P_+(x_{H^+}, x_t)\left[\frac{\sin^2\alpha}{M_{h^0}^2}\frac{(M_{H^+}^2 - M_{h_0}^2)}{M_W^2}\right. \\ &\qquad \left. + \frac{\cos^2\alpha}{M_{H^0}^2}\frac{(M_{H^+}^2 - M_{H_0}^2)}{M_W^2}\right], \\ C_P^{peng,2} &= -\frac{m_\ell}{2}\,\tan^2\beta\, P_+(x_{H^+}, x_t)\,\frac{1}{M_{A^0}^2}\left[\frac{M_{H^+}^2 - M_{A^0}^2}{M_W^2}\right]. \end{aligned} \tag{13}$$

The results in (12) and (13) involve the loop function

$$P_+(x,y) \;=\; \frac{y}{x-y}\left[\frac{x\,\log x}{x-1} - \frac{y\,\log y}{y-1}\right]. \tag{14}$$

### 3.3 Self-energies

Before we write down the result from the diagrams with self-energies in the external quark lines, we discuss how these contributions come into play. A treatment of flavor-changing self-energies has been proposed in [15,16] and analyzed in some detail in [17]. In these works flavor-changing self-energies have been discussed in a different context, the renormalization of the $W$-boson coupling to quarks. In [15–17] counterterms have been chosen in such a way that the flavor-changing self-energies vanish if either of the involved quarks is on-shell. For the down-type quarks these counterterms form two $3 \times 3$ matrices in flavor space, one for the left-handed quark fields and one for the right-handed ones, and similarly for the up-type quarks. It was argued in [16,17] that the anti-hermitian parts of the counterterm matrices for the left-handed fields can be absorbed into a renormalization of the CKM matrix, and the hermitian parts of the matrices can be interpreted as wave function renormalization matrices $Z^L_{ij}$ and $Z^R_{ij}$ with $i,j = d,s,b$ for our case of external down-type quarks.
However, it has also been argued [18] that the on-shell scheme of [16, 17] is not gauge invariant. In addition we find that the approach of [15–17] leads to an inconsistency in our calculation. We cannot cancel the anti-hermitian parts of the self-energies in the external lines with the counterterms for the CKM matrix, because unlike in the case of the $W$ coupling renormalization there is no tree-level coupling of a neutral scalar or vector boson to $\bar{b}d'$ to be renormalized. Hence we cannot absorb the anti-hermitian parts of the flavor-changing self-energy matrices into counterterms and they do contribute to our calculation.
The absorption of the hermitian parts into wave function counterterm matrices is optional, because the introduction of wave function counterterms only trivially shuffles self-energy contributions into vertex counterterms. It is most straightforward then to avoid the issue of counterterms altogether by simply calculating the fermion self-energy diagrams as they are shown in fig. 2. This calculation is straightforward because the internal $b$ quark line is off-shell and therefore it does not contribute to the 1-particle pole of the $s$ quark and needs not be truncated. It is crucial to note that one must start with $m_s \neq m_b$ in the diagrams with external self-energies in fig. 2 to properly account for the quark propagator $1/(m_b - m_s)$, and then take the limit $m_b, m_s \to 0$ (except in the $\tan\beta$-enhanced Higgs couplings, of course) at the end. FCNC transitions become

meaningless for degenerate quark masses, and one obtains an incorrect result if one starts with $m_s = m_b$ and regulates the propagator pole with an off-shell momentum $p$ with $p \to 0$. In this respect the Higgs exchange diagrams in fig. 2 differ from the situation with $\gamma$- or $Z$- exchanges, where both methods give the same correct result. Further we note that for $m_s \neq m_b$ one must include flavor-changing self-energies in external lines with a factor of 1 rather than of 1/2 as in the flavor-conserving case. This is due to the fact that flavor-conserving self-energies come from the residue of the one-particle pole, while in our approach flavor-changing self-energies are part of the non-truncated Green's function. By close inspection of the formulae in [17] one also recovers this "factor of 1 rule" from the expressions for the wave function renormalization matrices derived in [17].
There are two fermion self-energy diagrams that contribute in the 2HDM, one with a would-be Goldstone boson $G^+$ and one with the physical charged Higgs $H^+$. Their sum is ultraviolet-finite. This is different from the SM case, in which the UV divergence of the $G^+$ diagram cancels with the UV divergence of a SM Higgs vertex diagram involving a $G^+$ and a top quark in the loop. As in the penguin diagrams involving $H^+$ and $G^+$ in the loop, only the internal top quark contributions to the self-energy are relevant here, because the coupling of $H^+$ or $G^+$ to quarks is proportional to either of the quark masses and we neglect $m_s$. The self-energy diagrams add the following term to the Wilson coefficients:

$$\begin{aligned} C_S^{self} &= \frac{m_\ell}{2}\,\tan^2\beta\,(x_{H^+}-1)\,P_+(x_{H^+},x_t)\left[\frac{\sin^2\alpha}{M_{h^0}^2}+\frac{\cos^2\alpha}{M_{H^0}^2}\right], \\ C_P^{self} &= \frac{m_\ell}{2}\,\tan^2\beta\,(x_{H^+}-1)\,P_+(x_{H^+},x_t)\frac{1}{M_{A_0}^2}. \end{aligned} \tag{15}$$

## 3.4 2HDM Wilson coefficients and branching ratios

Adding (10), (12), (13) and (15) we obtain the 2HDM Wilson coefficients in (6):

$$C_S = C_P = \frac{m_\ell}{2M_W^2}\tan^2\beta\,\frac{\log r}{r-1}, \tag{16}$$

where $r \equiv x_{H^+}/x_t = M_{H^+}^2/m_t^2(m_t)$. Note that the dependence on the masses of the neutral Higgs bosons from the penguin and fermion self-energy diagrams has dropped out in their sum without invoking any relation between the mixing angle $\alpha$ and the Higgs masses. The result depends on only two of the 2HDM parameters: $\tan\beta$ and $M_{H^+}$.
The two hadronic matrix elements involved are related by the field equation of motion

$$\langle\, 0\,|\bar{b}\gamma^\mu\gamma_5 d'(x)|\, B_{d'}(P_{B_{d'}})\,\rangle \;=\; i\,f_{B_{d'}}\,P_{B_{d'}}^\mu e^{-i\,P_{B_{d'}}\cdot x}$$

$$\langle\, 0\,|\bar{b}\gamma_5 d'(x)|\, B_{d'}(P_{B_{d'}})\,\rangle \;=\; -i\, f_{B_{d'}}\, \frac{m^2_{B_{d'}}}{m_b + m_{d'}} e^{-i\,P_{B_{d'}}\cdot x}. \tag{17}$$

The resulting decay amplitude is

$$|\mathcal{A}| = \frac{G_F}{\sqrt{2}} \frac{\alpha_{EM} m_{B_{d'}} f_{B_{d'}}}{4\pi \sin^2\theta_W} \left| \xi_t \left[ \left( m_{B_{d'}} C_S \right) \bar{\ell}\ell + \left( m_{B_{d'}} C_P - \frac{2m_\ell}{m_{B_{d'}}} C_A \right) \bar{\ell}\gamma_5 \ell \right] \right|. \tag{18}$$

Here $f_{B_{d'}}$ is the $B_{d'}$ decay constant, normalized according to $f_\pi = 132$ MeV. The corresponding branching ratio is

$$\begin{aligned} \mathcal{B}(B_{d'} \to \ell^+\ell^-) \;&=\; \frac{G_F^2 \alpha_{EM}^2}{32\pi^2 \sin^4\theta_W} \frac{m^3_{B_{d'}} \tau_{B_{d'}} f^2_{B_{d'}}}{8\pi} |\xi_t|^2 \sqrt{1 - \frac{4m_\ell^2}{m^2_{B_{d'}}}} \\ &\quad \times \left[ \left( 1 - \frac{4m_\ell^2}{m^2_{B_{d'}}} \right) m^2_{B_{d'}} C_S^2 + \left( m_{B_{d'}} C_P - \frac{2m_\ell}{m_{B_{d'}}} C_A \right)^2 \right], \end{aligned} \tag{19}$$

where $\tau_{B_{d'}}$ is the $B_{d'}$ lifetime.
Numerically, the branching fractions are given by

$$\begin{aligned} \mathcal{B}(B_d \to \ell^+\ell^-) \;&=\; (3.0 \times 10^{-7}) \left[ \frac{\tau_{B_d}}{1.54\,\mathrm{ps}} \right] \left[ \frac{f_{B_d}}{210\,\mathrm{MeV}} \right]^2 \left[ \frac{|V_{td}|}{0.008} \right]^2 \frac{m_\ell^2}{m^2_{B_d}} \sqrt{1 - \frac{4m_\ell^2}{m^2_{B_d}}} \\ &\quad \times \left[ \left( 1 - \frac{4m_\ell^2}{m^2_{B_d}} \right) \left( \frac{m^2_{B_d} \tan^2\beta}{8M_W^2} \frac{\log r}{r-1} \right)^2 + \left( \frac{m^2_{B_d} \tan^2\beta}{8M_W^2} \frac{\log r}{r-1} - Y(x_t) \right)^2 \right], \\ \mathcal{B}(B_s \to \ell^+\ell^-) \;&=\; (1.1 \times 10^{-5}) \left[ \frac{\tau_{B_s}}{1.54\,\mathrm{ps}} \right] \left[ \frac{f_{B_s}}{245\,\mathrm{MeV}} \right]^2 \left[ \frac{|V_{ts}|}{0.040} \right]^2 \frac{m_\ell^2}{m^2_{B_s}} \sqrt{1 - \frac{4m_\ell^2}{m^2_{B_s}}} \\ &\quad \times \left[ \left( 1 - \frac{4m_\ell^2}{m^2_{B_s}} \right) \left( \frac{m^2_{B_s} \tan^2\beta}{8M_W^2} \frac{\log r}{r-1} \right)^2 + \left( \frac{m^2_{B_s} \tan^2\beta}{8M_W^2} \frac{\log r}{r-1} - Y(x_t) \right)^2 \right]. \end{aligned} \tag{20}$$

It is a well known property of the 2HDM that there exists a limit in which the particles $A^0$, $H^0$, and $H^+$ become very heavy and decouple from processes at the electroweak energy scale while $h^0$ remains light and its couplings approach those of the SM Higgs particle [19]. In the limit of large $M_{H^+}$, $C_P$ and $C_S$ fall as $M_{H^+}^{-2}$. Thus the deviation of the branching fractions from their SM prediction falls as $M_{H^+}^{-2}$ in the large $M_{H^+}$ limit, and the effects of the enlarged Higgs sector decouple.
Next we discuss the accuracy of the large $\tan\beta$ approximation. Subleading terms in $\tan\beta$ could be enhanced by powers of $m_t/m_b$ compared to our result in (16), as is

the case for the SM contribution. Such terms indeed occur, but they are suppressed by two powers of $\cot\beta$ compared to the SM terms in (16). Hence the formulae above are sufficient for all purposes; e.g. if $\tan\beta = 50$ the terms subleading in $\tan\beta$ give a correction only of $\mathcal{O}(2\%)$. If $\tan\beta$ is between a few and 15 the 2HDM corrections are small and experimentally hard to resolve, so that an error of order $\cot\beta$ is tolerable as well.

# 4 Comparison with other calculations

## 4.1 The analyses of He et al. and of Savage

In the paper of He, Nguyen and Volkas [3], the decays $B \to \ell^+\ell^-$, $B \to K\ell^+\ell^-$ and $b \to s\ell^+\ell^-$ are analyzed in both type-I and type-II 2HDMs. In [3], the only diagrams considered are the box diagram involving two charged Higgs bosons and the $A^0$ penguin involving $H^+$ and $W^+$ in the loop. Although the calculations of [3] are performed in the 't Hooft-Feynman gauge, the $A^0$ penguin involving $H^+$ and $G^+$ in the loop is not considered. Similarly, in the paper of Savage [4], the decay $B \to \mu^+\mu^-$ is considered in the 2HDM, with and without tree-level flavor-changing neutral Higgs couplings. Only the contribution of the $A^0$ penguin is considered. In both [3] and [4], several diagrams that are important at large $\tan\beta$ and required in order to obtain a gauge-independent result are neglected.

## 4.2 The analysis of Skiba and Kalinowski

In the paper of Skiba and Kalinowski [5], the decay $B_s \to \tau^+\tau^-$ is analyzed in the type-II 2HDM. In [5] additional penguin diagrams are considered that are not proportional to $\tan^2\beta$, but rather contain one or no powers of $\tan\beta$. We have neglected these contributions in our analysis, because they are not relevant for the interesting case of large $\tan\beta$. These additional penguin diagrams can be important for small values of $\tan\beta$ and in regions of the parameter space where some of the Higgs quartic couplings are very large resulting in large trilinear $H^+H^-H$ couplings ($H = h^0, H^0, A^0$).
Considering only terms proportional to $\tan^2\beta$, our results for the individual diagrams agree with those of [5], with two important exceptions. First, the authors of [5] incorrectly conclude that the box diagram involving $H^+$ and $W^+$ is negligible and therefore neglect it. If we neglect the box diagram, we find that the sum of the remaining contributions proportional to $\tan^2\beta$ is gauge-dependent. In the 't Hooft-Feynman gauge employed in [5] the omitted diagram gives the dominant contribution, affecting the nu-

merical result substantially. Second, our result for the $A^0$ penguin diagram involving $H^+$ and $G^+$ in the loop differs from that of [5] by a sign. Our sign is required for the gauge-independence of $C_P$.

### 4.3 The analyses of Huang et al. and Choudhury et al.

In the paper of Dai, Huang and Huang [6], the Wilson coefficients in (6) are calculated in the type-II 2HDM at large $\tan\beta$. As in our calculation, only the diagrams proportional to $\tan^2\beta$ are considered. However, the authors of [6] consider only the penguin and fermion self-energy diagrams with neutral Higgs boson exchange and neglect the box diagram with a $W$ and charged Higgs boson in the loop. Still, after leaving out the box diagram, our results for $C_S$ and $C_P$ in the 't Hooft-Feynman gauge do not agree with those of [6]. This is partly due to a typographical error in [6], which is corrected in [7,8]. There are two remaining discrepancies. First, our result for the $A^0$ penguin diagram involving $H^+$ and $W^+$ in the loop differs from that of [6] by a sign. Second, in [6] a contribution from the $h^0$ and $H^0$ penguin diagrams with two $H^+$ bosons in the loop is included. This diagram is included in [6] because it apparently receives a factor of $\tan\beta$ from the trilinear $H^+H^-H$ couplings ($H = h^0, H^0$). We argue in appendix A that the trilinear couplings should not be considered $\tan\beta$ enhanced. Therefore we conclude that the penguin diagram with two $H^+$ bosons in the loop should not be included in the $\mathcal{O}(\tan^2\beta)$ calculation because it is of subleading order in $\tan\beta$.
In [7, 8] the Wilson coefficients in (6) are calculated for supersymmetric models with large $\tan\beta$. If the diagrams involving supersymmetric particles are neglected, this calculation reduces to that for the type-II 2HDM with parameters constrained by supersymmetric relations. Again, in [7, 8] only the diagrams with neutral Higgs boson exchange are considered, and the box diagram with a charged Higgs boson and $W$ boson is not included. Leaving out the box diagram, our result for $C_S$ and $C_P$ in the 't Hooft-Feynman gauge does not agree with the non-SUSY part of that of [7, 8]. This discrepancy arises because our result for the penguin diagrams involving $H^+$ and $W^+$ in the loop differs from that of [7,8] by a sign. Once SUSY relations are imposed on the Higgs sector, it is clear that the penguin diagrams with two $H^+$ bosons in the loop are not of order $\tan^2\beta$, and the authors of [7, 8] have omitted these diagrams, as we did.
A final critical remark concerns the treatment of the renormalization group in the paper by Choudhury and Gaur [8]. They include an additional renormalization group factor to account for the running of the Wilson coefficients. Yet these authors have overlooked that the running of the (chiral) scalar quark current in $Q_S$ and $Q_P$ (see (7)) is compensated by the running of the $b$-quark mass multiplying the currents as explained in sect. 3. This leads to an underestimate of the Wilson coefficients by roughly 23%.

In conclusion, the papers in [3, 4], [5] and [6–8] disagree with each other, and our calculation does not agree with any of them. None of the results in [3–8] passes the test of gauge-independence and, in our opinion, each contains mistakes.

# 5 Phenomenology

As can be seen from the numerical coefficients in (20), $\mathcal{B}(B_s \to \ell^+\ell^-)$ is significantly larger than the corresponding branching fraction for $B_d$. This is due primarily to the relative sizes of $|V_{ts}|$ and $|V_{td}|$. As a result, even though the production rate of $B_s$ is three times smaller than that of $B_d$ at the Tevatron, the bounds on the leptonic branching fractions of $B_s$ are much closer to the SM predictions than those of $B_d$ [20]. For this reason we concentrate on the decays of $B_s$. Because of the suppression of the branching fractions by $m_\ell^2/m_B^2$, clearly the decay to $\tau$ pairs is the largest of the leptonic branching fractions in both the SM and the 2HDM. However, this decay is very difficult to reconstruct experimentally (due to the two missing neutrinos), and as a result the experimental limits on $B$ decays to $\tau$ pairs are very weak. Therefore in our numerical analysis we focus on the decay $B_s \to \mu^+\mu^-$, for which the experimental bound is the closest to the SM prediction. The best experimental bound comes from CDF [20], where one candidate event for $B \to \mu^+\mu^-$ has been reported; this event was consistent with the expected background and lay in the overlapping part of the search windows for $B_d$ and $B_s$. The corresponding 95% confidence level upper bound on the $B_s \to \mu^+\mu^-$ branching fraction is [20]

$$\mathcal{B}(B_s \to \mu^+\mu^-) < 2.6 \times 10^{-6} \qquad (\text{expt}). \tag{21}$$

The SM prediction for the branching fraction is

$$\mathcal{B}(B_s \to \mu^+\mu^-) = 4.1 \times 10^{-9} \qquad (\text{SM}), \tag{22}$$

where we have taken the central values for all inputs in (20) and ignored the 2HDM contributions as well as the errors in the hadronic parameters.

Because the 2HDM Wilson coefficients in (16) depend on only two of the parameters of the 2HDM, $\tan\beta$ and $M_{H^+}$, the behavior of the result in different parts of parameter space is easy to understand. In regions of the parameter space with a large 2HDM contribution to $\mathcal{B}(B_{d'} \to \ell^+\ell^-)$ compared to the SM contribution, we may neglect $Y(x_t)$ in (20). Then the result is particularly simple: the branching fractions are proportional to $\tan^4\beta \, \log^2 r/(r-1)^2$.

We can see from (20) and the value of $Y(x_t)$ given in (9) that the interference between the SM and 2HDM contributions to the branching fractions is destructive. The effect of

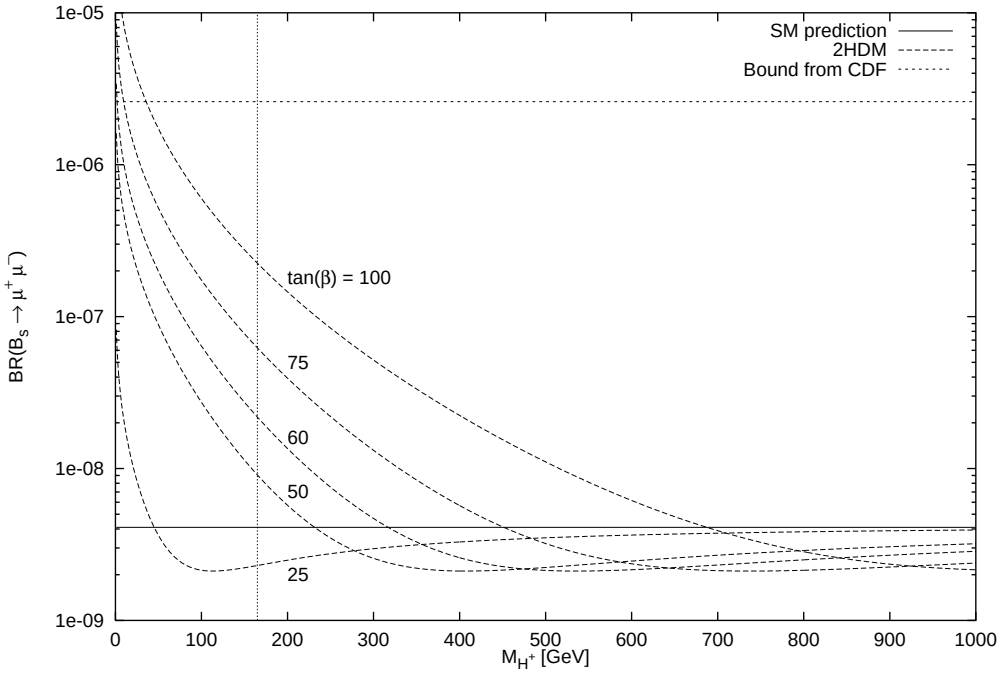


Figure 3: $\mathcal{B}(B_s \to \mu^+\mu^-)$ in the 2HDM as a function of $M_{H^+}$ for $\tan\beta = 100$, 75, 60, 50 and 25. For comparison we show the current experimental bound [20] and the SM prediction for the branching fraction. The vertical line is the lower bound on $M_{H^+}$ in the type-II 2HDM from $b \to s\gamma$ [21].

the destructive interference can clearly be seen in fig. 3. In fig. 3 we plot the predicted value of $\mathcal{B}(B_s \to \mu^+\mu^-)$ in the 2HDM as a function of $M_{H^+}$, for various values of $\tan\beta$. For comparison we show the constraint on $M_{H^+}$ from $b \to s\gamma$ [21], obtained from the current 95% confidence level experimental upper bound of $\mathcal{B}(b \to s\gamma) < 4.5 \times 10^{-4}$ from the CLEO experiment. For very large $\tan\beta$ and relatively light $H^+$, the 2HDM contribution dominates and the branching fraction is significantly enhanced compared to its SM value. As the 2HDM contribution becomes smaller due to increasing $M_{H^+}$ or decreasing $\tan\beta$, the branching fraction drops, eventually falling below the SM prediction due to the destructive interference. If we ignore the kinematical factor of $(1-4m_\ell^2/m_{B_{d'}}^2)$ in front of $C_S$ in (19) (which is a good approximation for $B_{d'} \to \mu^+\mu^-$ but not for $B_{d'} \to \tau^+\tau^-$) then we can easily show that the branching fraction in the 2HDM crosses the SM value when

$$\frac{m_{B_s}^2 \tan^2\beta}{8M_W^2}\frac{\log r}{r-1} = Y(x_t), \tag{23}$$

and reaches a minimum of half the SM value when

$$\frac{m_{B_s}^2 \tan^2\beta}{8M_W^2}\frac{\log r}{r-1} = \frac{1}{2}Y(x_t). \tag{24}$$

These correspond to $\tan^2\beta \log r/(r-1) = 1790$ and 893, respectively. As a numerical example, taking $\tan\beta = 60$ and $M_{H^+} = 175$ GeV (500 GeV), we find $\mathcal{B}(B_s \to \mu^+\mu^-) = 1.8 \times 10^{-8}$ ($2.1 \times 10^{-9}$).

In fig. 4 we plot the regions of $M_{H^+}$ and $\tan\beta$ parameter space that will be probed as the sensitivity to the decay $B_s \to \mu^+\mu^-$ improves at the Tevatron Run II. The contours shown (from left to right) were chosen as follows. The current upper bound on $\mathcal{B}(B_s \to \mu^+\mu^-)$ is $2.6 \times 10^{-6}$ from CDF [20] with about 100 pb$^{-1}$ of integrated luminosity. This bound excludes a small region of parameter space with very high $\tan\beta$ and very light $H^+$, shown by the solid line at the far left of fig. 4. Such low $H^+$ masses are already excluded by the constraint from $b \to s\gamma$ [21]. The rest of the contours in fig. 4 show the regions that we expect to be probed at the Tevatron Run II and extended Run II with various amounts of integrated luminosity, assuming that the background for this process remains negligible. In this case the sensitivity to the branching fraction should scale with the luminosity. If there is background however, then the sensitivity will scale only with the square root of the luminosity. With 2 fb$^{-1}$ from each of the two detectors, the sensitivity should improve by a factor of 40 over the current sensitivity, to $6.5 \times 10^{-8}$, shown by the short dashes in fig. 4. For the values of $\tan\beta$ that we consider, this sensitivity will still only probe values of $M_{H^+}$ already excluded by $b \to$

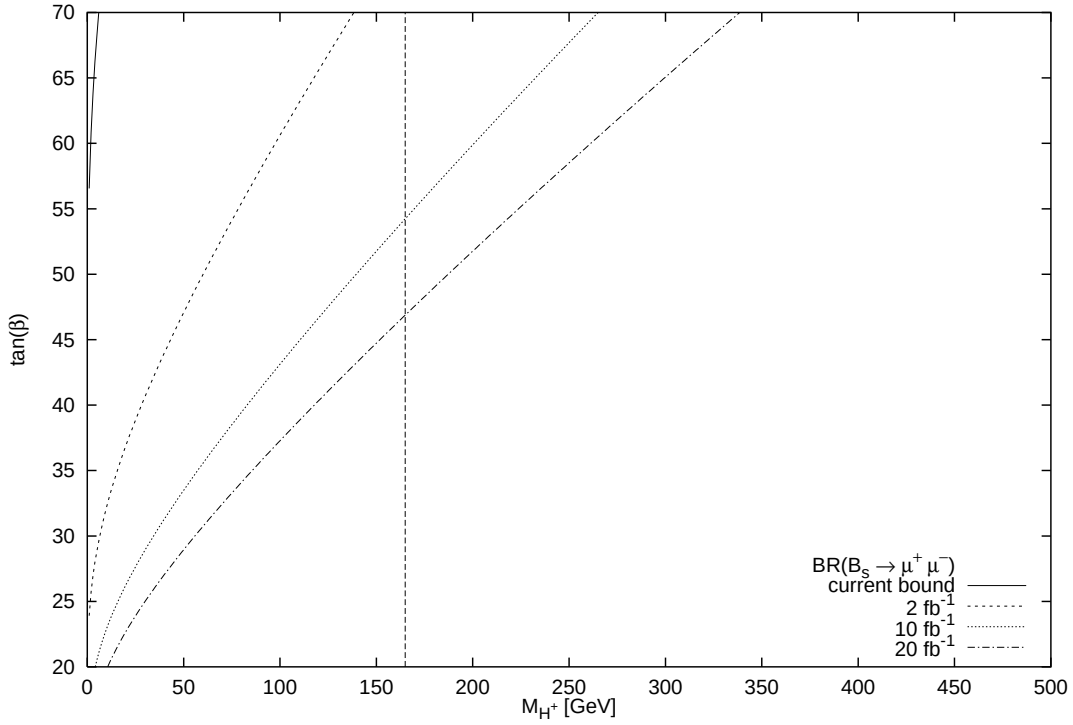


Figure 4: Regions of $M_{H^+}$ and $\tan\beta$ parameter space probed by measurements of $\mathcal{B}(B_s \to \mu^+\mu^-)$. Contours are chosen as described in the text. The vertical dashed line is the present lower bound on $M_{H^+}$ in the type-II 2HDM from $b \to s\gamma$ [21].

$s\gamma$. We also show two contours for the expected sensitivity with 10 fb$^{-1}$ and 20 fb$^{-1}$ of integrated luminosity per detector (dotted and dot-dashed lines in fig. 4, respectively). These correspond to an extended Run II of the Tevatron. With 10 fb$^{-1}$ we expect the sensitivity to reach a branching fraction of $1.3\times10^{-8}$, allowing one to begin to probe $H^+$ masses above the current bound from $b\to s\gamma$ for $\tan\beta > 54$. With 20 fb$^{-1}$ we expect a reach of $6.5\times10^{-9}$, less than a factor of two above the predicted SM branching fraction. This would allow one to probe $H^+$ masses above the current bound from $b\to s\gamma$ for $\tan\beta > 47$. In particular, for $\tan\beta = 60$, a non-observation of $B_s\to\mu^+\mu^-$ at this sensitivity would rule out $H^+$ lighter than 260 GeV.

Looking farther into the future, the experiments at the CERN LHC expect to observe the following numbers of signal (background) events for $B_s\to\mu^+\mu^-$ after three years of running at low luminosity, assuming the SM branching fraction [22]: ATLAS: 27 (93); CMS: 21 (3); and LHCb: 33 (10). Since the suppression of this branching fraction in the 2HDM is at most a factor of two, the LHC experiments will be able to observe this decay for any configuration of the 2HDM at large $\tan\beta$. For e.g. $\tan\beta = 60$ and $M_{H^+} < 285$ GeV, the branching fraction in the 2HDM is enhanced by 30% or more compared to the SM. Similarly, for $\tan\beta = 60$ and 375 GeV $< M_{H^+} <$ 1 TeV, the branching fraction is suppressed by 30% or more compared to the SM[3]. In these regions, we expect the LHC to be able to distinguish the 2HDM from the SM. In the region of large $M_{H^+}$, the dependence on $M_{H^+}$ is very weak; hence the LHC measurement will give powerful constraints on $\tan\beta$ in the large $\tan\beta$ region.

We have made no attempt to simulate the experimental background for this decay in order to obtain an accurate estimate of the reach of the Tevatron Run II. Neither have we taken into account the theoretical uncertainty. We expect the largest theoretical uncertainty to come from uncertainties in the input parameters, primarily the $B$ meson decay constants and CKM matrix elements in (20). These uncertainties will be reduced as the $B$ physics experiments progress and lattice calculations improve. Also QCD corrections to the 2HDM contribution will arise at NLO and require the calculation of two-loop diagrams. In the SM, the NLO corrections increase the decay amplitude by about 3%, and therefore increase the branching fraction by about 6%. We expect the NLO corrections to the 2HDM contribution to be of the same order, in which case our conclusions are not significantly modified.

In order to evaluate the usefulness of $B_s\to\mu^+\mu^-$ as a probe of the 2HDM, we must compare it to other measurements that constrain the 2HDM in the large $\tan\beta$ regime. As the statistics of $B$ physics experiments improve, the measurement of $b\to s\gamma$ will improve as well. If $B_s\to\mu^+\mu^-$ is to be a useful probe of the 2HDM, it must be sen-

[3]We do not consider charged Higgs masses larger than 1 TeV for naturalness reasons.

sitive to a range of parameter space not already explored by $b \to s\gamma$ at each integrated luminosity. Fortunately, $B_s \to \mu^+\mu^-$ is complementary to $b \to s\gamma$ because of the different dependence on $\tan\beta$. While the 2HDM contributions to $b \to s\gamma$ are independent of $\tan\beta$ for $\tan\beta$ larger than a few, the 2HDM contributions to $B_s \to \mu^+\mu^-$ depend sensitively on $\tan\beta$. This makes $B_s \to \mu^+\mu^-$ an especially sensitive probe of the 2HDM in the large $\tan\beta$ regime, while $b \to s\gamma$ will remain more sensitive for moderate and small $\tan\beta$. Finally, a fit to the $Z$ decay data in the 2HDM [23] puts weak constraints on the $H^+$ mass for very large $\tan\beta$: $M_{H^+} > 40$ GeV at 95% confidence level for $\tan\beta = 100$. The fit gives no constraint for $\tan\beta < 94$.

# 6 Conclusions

In this paper we have analyzed the decays $B_{d'} \to \ell^+\ell^-$ in the type-II 2HDM with large $\tan\beta$. Although these decays have been studied in a 2HDM before, the previous analyses omitted the box diagram involving $W$ and $H^+$, which is the dominant contribution at large $\tan\beta$ in the 't Hooft-Feynman gauge and is needed for gauge independence. We showed that when all the contributions are properly included in the large $\tan\beta$ limit, the resulting expressions for the branching fractions are quite simple and depend only on $\tan\beta$ and the charged Higgs mass. These 2HDM contributions can enhance or suppress the branching fractions by a significant amount compared to their SM values, providing tantalizing search possibilities with the potential to probe large parts of the large $\tan\beta$ parameter space of the 2HDM. We have focused in our numerical analysis on $B_s \to \mu^+\mu^-$, for which the the experimental sensitivity is best. We find that for reasonable values of $\tan\beta$ up to 60 and charged Higgs masses above the lower bound set by $b \to s\gamma$, $\mathcal{B}(B_s \to \mu^+\mu^-)$ can be increased by up to a factor of five above its SM expectation or suppressed by up to a factor of two, depending on the charged Higgs mass. Although very high statistics will be needed to observe this decay, it promises to be an experimentally and theoretically clean probe of new Higgs physics.

# Acknowledgments

We are grateful to Jan Kalinowski and Witold Skiba for helpful discussions, and to Jonathan Lewis for discussions on the reach of the Tevatron in Run II. We would also like to thank the conveners of the B-Physics at Run II Workshop at Fermilab for facilitating useful interaction among theorists and experimentalists. Finally we owe a debt of gratitude to Piotr Chankowski and Łucja Sławianowska for pointing out an error in the

relative sign between the SM- and 2HDM-induced contributions to the decay rate in an earlier version of this manuscript, and for confirming our result for the 2HDM Wilson coefficients.

# A Trilinear Higgs couplings

The trilinear $H^+H^-H$ couplings ($H = h^0, H^0$) for the non-supersymmetric 2HDM were first presented in [5]. These couplings depend strongly on the model considered. For the most general CP-conserving 2HDM with natural flavor conservation, the $H^+H^-H$ couplings are given by $igQ_H/M_W$, where

$$\begin{aligned} Q_{h^0} &= -v_{SM}^2 \left[\sin(\beta-\alpha)(2\lambda_3+\lambda_4) - \sin\beta\cos\beta\cos(\alpha+\beta)\lambda_5 \right. \\ &\qquad \left. +2\sin\beta\cos\beta\left(-\sin\alpha\sin\beta\lambda_1 + \cos\alpha\cos\beta\lambda_2\right)\right] \\ Q_{H^0} &= -v_{SM}^2 \left[\cos(\beta-\alpha)(2\lambda_3+\lambda_4) - \sin\beta\cos\beta\sin(\alpha+\beta)\lambda_5 \right. \\ &\qquad \left. +2\sin\beta\cos\beta\left(\cos\alpha\sin\beta\lambda_1 + \sin\alpha\cos\beta\lambda_2\right)\right]. \end{aligned} \tag{25}$$

The $H^+H^-A^0$ coupling is zero. Here $v_{\rm SM} = 174$ GeV is the SM Higgs vev, and the $\lambda_i$ are the scalar quartic couplings of the Higgs potential given in [9]. To write these couplings in terms of Higgs masses and mixing angles, one must make an assumption to eliminate one of the independent $\lambda_i$. In [5], formulae are presented for the two cases $\lambda_1 = \lambda_2$ and $\lambda_5 = \lambda_6$. The formulae in (25) agree with [5] in these two cases.
At large $\tan\beta$, (25) reduces to

$$\begin{aligned} Q_{h^0} &\simeq -v_{\rm SM}^2 \cos\alpha(2\lambda_3+\lambda_4)\left[1+\mathcal{O}(\cot\beta)\right] \\ Q_{H^0} &\simeq -v_{\rm SM}^2 \sin\alpha(2\lambda_3+\lambda_4)\left[1+\mathcal{O}(\cot\beta)\right]. \end{aligned} \tag{26}$$

These couplings are not enhanced at large $\tan\beta$.
Considering instead the case $\lambda_1 = \lambda_2$ and writing the trilinear couplings in terms of Higgs masses and mixing angles, we find at large $\tan\beta$,

$$\begin{aligned} Q_{h^0} &\simeq -\tfrac{1}{2} M_{H^0}^2 \tan\beta\cos^2\alpha\sin\alpha\left[1+\mathcal{O}(\cot\beta)\right] \\ Q_{H^0} &\simeq \tfrac{1}{2} M_{h^0}^2 \tan\beta\cos\alpha\sin^2\alpha\left[1+\mathcal{O}(\cot\beta)\right]. \end{aligned} \tag{27}$$

Naively, one would conclude that these couplings are enhanced at large $\tan\beta$. This is incorrect because the angle $\alpha$ depends on $\tan\beta$. At large $\tan\beta$ we have

$$\tan 2\alpha = \frac{2(4\lambda_3+\lambda_5)}{\lambda_5 - 4(\lambda_2+\lambda_3)}\cot\beta\left[1+\mathcal{O}(\cot^2\beta)\right]. \tag{28}$$

Thus for generic values of the $\lambda_i$, $\sin\alpha \sim \cot\beta$, and the $\tan\beta$ enhancement in (27) is cancelled.

# References

[1] D. Boutigny *et al.*, *BaBar technical design report*, SLAC-R-0457; M. T. Cheng *et al*. (Belle collaboration), *A study of CP violation in B meson decays: Technical design report*, BELLE-TDR-3-95; K. Pitts (for Fermilab D0 and CDF collaborations), Proceedings 4th Workshop on Heavy Quarks at Fixed Target (HQ 98), Batavia, USA, 1998; P. Krizan *et al.*, *HERA-B, an experiment to study CP violation at the HERA proton ring using an internal target*, Nucl. Instrum. Meth. **A351**, 111 (1994); The ATLAS Collaboration, *ATLAS Technical Proposal*, CERN/LHCC/94-43; The CMS Collaboration, *CMS Technical Proposal*, CERN/LHCC/94-38; The LHCb Collaboration, *LHCb Technical Proposal*, CERN/LHCC/98-4.

[2] H. Fritzsch and P. Minkowski, Annals Phys. **93** (1975) 193. M. S. Chanowitz, J. Ellis and M. K. Gaillard, Nucl. Phys. **B128** (1977) 506. H. Georgi and D. V. Nanopoulos, Nucl. Phys. **B155** (1979) 52.

[3] X. G. He, T. D. Nguyen and R. R. Volkas, Phys. Rev. D **38**, 814 (1988).

[4] M. J. Savage, Phys. Lett. B **266**, 135 (1991).

[5] W. Skiba and J. Kalinowski, Nucl. Phys. **B404**, 3 (1993).

[6] Y.-B. Dai, C.-S. Huang and H.-W. Huang, Phys. Lett. B **390**, 257 (1997).

[7] C.-S. Huang and Q.-S. Yan, hep-ph/9803366; C.-S. Huang, W. Liao and Q.-S. Yan, Phys. Rev. D **59**, 011701 (1999).

[8] S. R. Choudhury and N. Gaur, Phys. Lett. B **451**, 86 (1999).

[9] J. F. Gunion, H. E. Haber, G. Kane and S. Dawson, *The Higgs Hunter's Guide* (Addison-Wesley, Reading, MA, 1990); errata hep-ph/9302272.

[10] S. L. Glashow and S. Weinberg, Phys. Rev. D **15**, 1958 (1977); E. A. Paschos, Phys. Rev. D **15**, 1966 (1977).

[11] T. Inami and C. S. Lim, Prog. Theor. Phys. **65**, 297 (1981) [erratum **65**, 1772 (1981)].

[12] B. Grządkowski and P. Krawczyk, Z. Phys. C **18**, 43 (1983).

[13] P. Krawczyk, Z. Phys. C **44**, 509 (1989).

[14] G. Buchalla and A. J. Buras, Nucl. Phys. **B400**, 225 (1993); M. Misiak and J. Urban, Phys. Lett. B **451**, 161 (1999).

[15] K. I. Aoki, Z. Hioki, M. Konuma, R. Kawabe and T. Muta, Prog. Theor. Phys. Suppl. **73**, 1 (1982).

[16] W. J. Marciano and A. Sirlin, Nucl. Phys. **B93**, 303 (1975).

[17] A. Denner and T. Sack, Nucl. Phys. **B347**, 203 (1990).

[18] P. Gambino, P. A. Grassi and F. Madricardo, Phys. Lett. B **454**, 98 (1999), hep-ph/9811470.

[19] H. E. Haber and Y. Nir, Nucl. Phys. **B335**, 363 (1990); H. E. Haber, in *Budapest Electroweak 1994*, F. Csikor and G. Pocsik (Ed.) (World Scientific, Singapore, 1995), 1, hep-ph/9501320.

[20] F. Abe *et al.* (CDF collaboration), Phys. Rev. D **57**, 3811 (1998).

[21] J. L. Hewett, Phys. Rev. Lett. **70**, 1045 (1993); V. Barger, M. Berger and R. J. N. Phillips, Phys. Rev. Lett. **70**, 1368 (1993); S. Bertolini, F. Borzumati and A. Masiero, "Probing new physics in FCNC B decays and oscillations", in *B Decays*, S. Stone (Ed.) (World Scientific, Singapore, 1992), 458-478 (1st Edition) and (1994), 620-643 (2nd Edition); M. S. Alam *et al.* (CLEO collaboration), CLEO CONF 98-17, talk presented at XXIX International Conference on High Energy Physics, Vancouver, Canada, 23-29 July 1998; F. M. Borzumati and C. Greub, hep-ph/9810240.

[22] P. Ball *et al.*, hep-ph/0003238.

[23] O. Lebedev, W. Loinaz and T. Takeuchi, hep-ph/0002106.